ELSEVIER

27 October 1997

PHYSICS LETTERS A

Physics Letters A 235 (1997) 139–144

Discontinuous pattern of cumulative separation between orbits of chaotic transient

V. Paar [1], N. Pavin

Department of Physics, Faculty of Science, University of Zagreb, Zagreb, Croatia

Received 5 December 1996; revised manuscript received 21 April 1997; accepted for publication 6 August 1997
Communicated by A.P. Fordy

Abstract

The logistic map at $r = 4$ is modified in a narrow interval, stabilizing a low-period unstable periodic orbit and generating transient chaos. The cumulative separation Δ between closely lying orbits is proportional to their initial separation ϵ for $\epsilon < \epsilon_c$, while for $\epsilon > \epsilon_c$ it is scattered within a band with ϵ-independent average, where ϵ_c is a critical value of initial separation. The pattern of (ϵ, Δ)-diagram is proposed for characterization of transient chaos. On the basis of these considerations, the concept of the uncertainty exponent is extended to the case of transient chaos. © 1997 Elsevier Science B.V.

PACS: 05.45.+b
Keywords: Transient chaos; Modified logistic map; Controlling chaos; Cumulative separation of orbits; Unstable periodic orbits; Average lifetime; Uncertainty exponent

Transient chaos can often be observed in numerical simulations [1–21]. In systems exhibiting transient chaos there exists a chaotic repeller, an invariant set with measure zero basin of attraction, together with an attractor which is often periodic.

Transiently chaotic orbits starting from randomly chosen initial points approach the attractor, but prior to reaching it, they might come close to the strange repeller and stay in its vicinity for some time (i.e. for a number of iteration steps). This results in the appearance of chaotic motion with an average lifetime which is a basic characteristic of the repeller [1,21]. However, it is worth emphasizing [1] that the existence of a well-defined average lifetime of transients does not imply their chaoticity. Orbits around the repeller have positive effective Lyapunov exponents due to its repelling feature. Therefore, in order to decide if the transients are really chaotic or not one needs more information. To this end, in characterization of transients additional criteria have been considered, such as construction of the repeller, natural invariant distribution on the repeller and power spectra [1].

Transient chaos has been investigated previously for single-humped one-dimensional maps, such as, for example, the logistic map at $r > 4$ [1,18,20,21]. Here we modify the logistic map at $r = 4$ in a narrow interval containing a particular low-period unstable periodic orbit, and in this way we stabilize it. This method is related to the problematics of controlling chaos [22], which has received much attention in recent years.

A famous case of a one-dimensional map

[1] E-mail: paar@mahazu.hazu.hr.

PII S0375-9601(97)00650-6

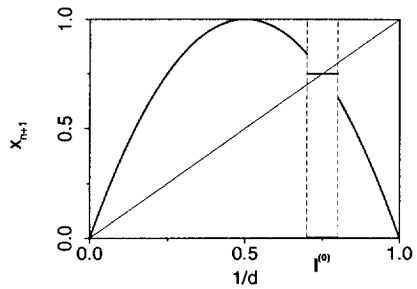

Fig. 1. Map (3) at $\xi = \frac{3}{4}$, $d = 0.1$.

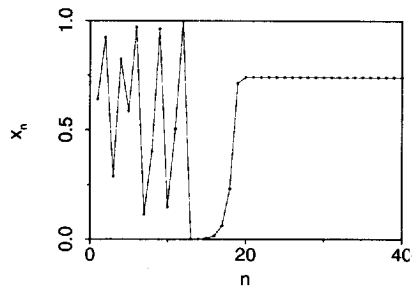

Fig. 2. Transiently chaotic orbit of the map (3) at $\xi = \frac{3}{4}$, $d = 0.1$, $x_0 = 0.2$.

$$x_{n+1} = f(x_n), \tag{1}$$

which produces permanent chaos, is the logistic map at $r = 4$ [21,23,24], which is given by

$$f(x) = 4x(1-x). \tag{2}$$

Let us now consider the modified logistic map defined on the unit interval I by

$$\begin{aligned} f(x) &= 4x(1-x), \quad x \notin I^{(0)}, \\ &= 4\xi(1-\xi), \quad x \in I^{(0)}, \end{aligned} \tag{3}$$

where $I^{(0)}$ is a narrow subinterval $[\xi - \frac{1}{2}d, \xi + \frac{1}{2}d]$ within the unit interval I. In the interval $I_c \equiv I - I^{(0)}$ this map coincides with the logistic map at $r = 4$, while in the narrow interval $I^{(0)}$ of width d at the position $x = \xi$ the map has a constant value $4\xi(1-\xi)$.

The logistic map at $r = 4$ is chaotic in the unit interval I, with an embedded infinite number of unstable periodic orbits [21]. At the point of intersection of the function (2) and diagonal, the map (2) has an unstable periodic orbit of period-1. On the other hand, modifying the logistic map at $r = 4$ in a small interval $I^{(0)}$, as done for the map (3) at $\xi = \frac{3}{4}$, this unstable periodic point is stabilized, becoming a period-1 attractor (Fig. 1) within the interval $I^{(0)}$.

Taking initial points in the interval $I_c \equiv I - I^{(0)}$, the orbits of the map (3) are, for a certain initial number of N_c iteration steps (that depends on x_0), similar to permanently chaotic orbits of the logistic map (2), but after the N_c iteration steps they are mapped into interval $I^{(0)}$ with a period-1 attractor at $x = \frac{3}{4}$. An example of such an orbit is shown in Fig. 2.

In the first iteration step the preimages $I^{(1)}$ of $I^{(0)}$ escape from I_c, in the second step the preimages $I^{(2)}$ of $I^{(1)}$, etc. Finally, the remaining invariant set in I_c is a chaotic repeller. Thus, the map (3) at $\xi = \frac{3}{4}$ is characterized by the chaotic repeller and the period-1 attractor.

In the case of the logistic map at $r = 4$ (Eq. (2)) the cumulative separation between orbits after N iterations is approximately proportional to ϵ,

$$\begin{aligned} &\sum_{n=0}^{N} \tfrac{1}{2}[\,|x_n(x_0+\epsilon) - x_n(x_0)| \\ &\quad + |x_n(x_0-\epsilon) - x_n(x_0)|\,] \approx k_c\epsilon \end{aligned} \tag{4}$$

with

$$k_c(N) = 2^{N+1} - 1. \tag{5}$$

In Eq. (4), the terms $x_n(x_0+\epsilon)$, $x_n(x_0-\epsilon)$ and $x_n(x_0)$ are the nth iterates of the initial points $x_0+\epsilon$, $x_0-\epsilon$ and x_0, respectively.

In this paper we calculate the cumulative separation between transiently chaotic orbits for the map (3) at $\xi = \frac{3}{4}$

$$\begin{aligned} \Delta \equiv &\sum_{n=0}^{N_\infty} \tfrac{1}{2}[\,|x_n(x_0+\epsilon) - x_n(x_0)| \\ &+ |x_n(x_0-\epsilon) - x_n(x_0)|\,] \end{aligned} \tag{6}$$

in dependence on the initial separation ϵ. Here N_∞ is much larger than the reciprocal value of the escape rate. In the present case we take $N_\infty = 1000$. In Fig. 3a the (ϵ, Δ)-diagram associated with $x_0 = 0.2$ is presented in the log–log plot.

It is seen that up to a certain critical value of ϵ, denoted by ϵ_c, the dependence of $\log\Delta$ on $\log\epsilon$ is linear,

$$\log\Delta = \log a + b\log\epsilon,$$

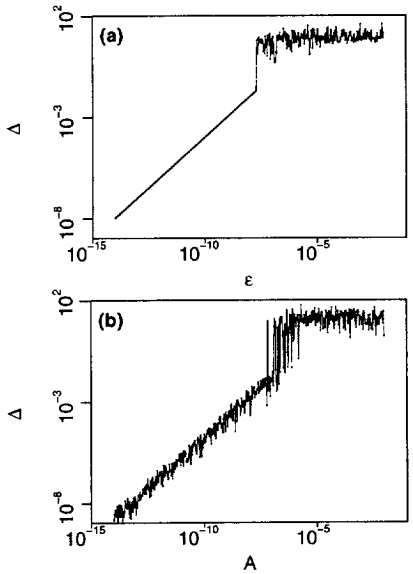

Fig. 3. (a) Log–log plot of $\Delta \equiv \sum_{n=0}^{N_\infty} \frac{1}{2}[|x_n(x_0+\epsilon)-x_n(x_0)| + |x_n(x_0-\epsilon)-x_n(x_0)|]$ versus ϵ for the map (3). Parameters ξ, d and x_0 are the same as in Fig. 2 and $N_\infty = 1000$. (b) Log–log plot of Δ versus noise amplitude A in the case of adding noise to the r.h.s. of Eq. (3) for $x_0 = 0.2$.

that is $\Delta = a\epsilon^b$, where a and b are constant parameters. Fitting this expression to the results of our calculation we obtain $b = 1.000001 \pm 0.000002$, i.e. $b = 1$ within the limits of precision. Denoting the coefficient a, associated with the modified logistic map (3), by k_{TC} in analogy to the relation (4) for the logistic map at $r = 4$ (2) we obtain

$$\Delta = k_{TC}\epsilon. \tag{7}$$

However, at $\epsilon = \epsilon_c$ a discontinuous transition appears in the Δ versus ϵ dependence: values of Δ are scattered within a horizontal band, with an average value which is approximately independent on ϵ. A closer look reveals a finer substructure within this band, bearing similarity to the time map for lifetimes of chaotic transients in dependence on the initial position x_0.

Our calculations for ϵ_c and k_{TC} are performed for initial conditions $x_0 \in I - I^{(0)}$. For completeness, we note that in the case $x_0 \in I^{(0)}$ there is $\Delta = \epsilon$, $k_{TC} = 1$. In this case, the value of ϵ_c is determined from the distance of x_0 to the nearer boundary of the interval $I^{(0)}$.

To get a closer insight into the nature of the (ϵ, Δ)-diagram in Fig. 3a we have investigated the modification of the map (3) by adding a noise term on the r.h.s. of Eq. (3). The dependence of Δ on the noise amplitude A is illustrated in Fig. 3b. The straight line for $\epsilon < \epsilon_c$ from Fig. 3a is then replaced by a band of scattered points of the same slope while the horizontal band for $\epsilon > \epsilon_c$ remains similar as before, but the scattering of points appears more random. This reflects a degree of robustness of the pattern of (ϵ, Δ)-diagram from Fig. 3a.

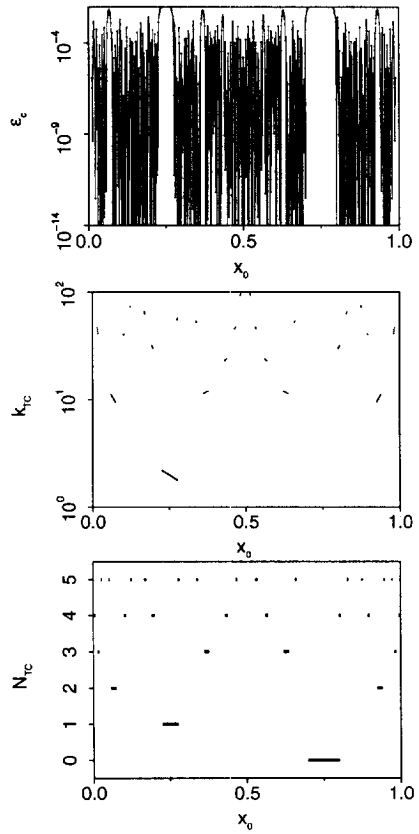

Fig. 4. Top: Lin–log plot of critical value ϵ_c in dependence on the initial position x_0. Other parameters are the same as in Fig. 3a. Middle: Lin–log plot of k_{TC} versus x_0. Bottom: Number of iteration steps N_{TC} versus x_0.

Let us now investigate the corresponding critical values ϵ_c and k_{TC}. In Fig. 4 the values of ϵ_c and k_{TC} are shown in dependence on the initial position x_0. It is seen that the (x_0, k_{TC})-diagram bears qualitative similarity to the (x_0, N_{TC})-diagram also shown in Fig. 4, indicating a relation between k_{TC} and N_{TC} (length of chaotic transient). Comparing the upper two figures in Fig. 4, we see that $\epsilon_c(x_0^{max})$ and $k_{TC}(x_0^{max})$, are

Table 1
Comparison of the values $k_c(N_{TC}) = 2^{N_{TC}+1} - 1$ (Eq. (5)), and the values of the coefficient k_{TC} determined from the (ϵ, Δ)-diagram (Eq. (7)). Results are shown for orbits with several values of initial position x_0 for the map (3) at $\xi = \frac{3}{4}$, $d = 0.1$. N_{TC} is the length of chaotic transient (the number of iteration steps before the orbit ends in the interval $I^{(0)}$). The calculated values of k_{TC} are presented in the form $2^x - 1$

x_0	N_{TC}	$k_c(N_{TC})$	k_{TC}
0.05	22	$2^{23} - 1$	$2^{23.78} - 1$
0.10	19	$2^{20} - 1$	$2^{20.32} - 1$
0.20	19	$2^{20} - 1$	$2^{19.90} - 1$
0.30	38	$2^{39} - 1$	$2^{38.88} - 1$
0.40	21	$2^{22} - 1$	$2^{21.60} - 1$
0.45	10	$2^{11} - 1$	$2^{10.61} - 1$
0.55	10	$2^{11} - 1$	$2^{10.60} - 1$
0.65	10	$2^{11} - 1$	$2^{10.74} - 1$
0.95	22	$2^{23} - 1$	$2^{23.80} - 1$

approximately inversely proportional to each other,

$$\epsilon_c(x_0^{max}) k_{TC}(x_0^{max}) \approx \kappa, \tag{8}$$

where κ is a constant value. Here x_0^{max} denotes a value of x_0 at each of the pronounced maxima of ϵ_c in dependence on x_0. Including 20 maxima of largest width we get $\kappa = 0.089 \pm 0.005$. However, outside of positions of maxima the inverse proportionality of ϵ_c and k_{TC} is less pronounced because of the difference in shapes of the $\epsilon_c(x_0)$ and $k_{TC}(x_0)$ dependences.

On the other hand, the coefficient k_{TC} is closely related to the length of the chaotic transient N_{TC}, as seen by comparing the two lower figures in Fig. 4.

In order to clarify this point, the calculated value of k_{TC} is given in Table 1 for several typical values of the initial position x_0. For comparison, the corresponding values of $k_c(N_{TC}) = 2^{N_{TC}+1} - 1$ are also given (which would correspond to the first N_{TC} steps of permanent chaos). Here N_{TC} denotes the length of the corresponding chaotic transient, which is given in the second column of Table 1. We obtain the result

$$k_{TC} \approx k_c(N_{TC}), \tag{9}$$

which reveals that during its lifetime of length N_{TC} a transiently chaotic orbit has a similar (ϵ, Δ)-diagram as a permanently chaotic orbit during the first N_{TC} iteration steps.

Let us now consider how the escape rate depends on the width d of the interval $I^{(0)}$. The Frobenius–

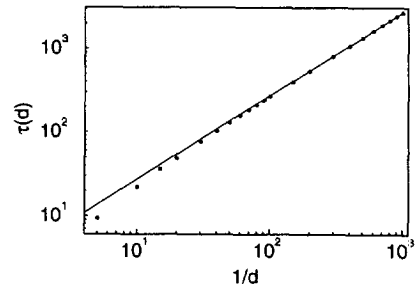

Fig. 5. Average lifetime of orbits of the map (3) in dependence on the inverse value of width, $1/d$. The calculated values (solid circles) are compared to the theoretical prediction of Eq. (11) (solid line).

Perron equation, which was previously applied to the chaotic transients of the logistic map at $r > 4$ [25], determines for small d the lifetime, which is denoted by τ_{FP},

$$\left(1 - \frac{1}{\pi\sqrt{\xi(1-\xi)}} d\right)^{\tau_{FP}} \approx \frac{1}{e}.$$

Therefrom we obtain

$$\tau_{FP} \approx \frac{\pi\sqrt{\xi(1-\xi)}}{d}$$

and for $\xi = \frac{3}{4}$, employed in this paper, we have

$$\tau_{FP} \approx \frac{\pi\sqrt{3}}{4}\frac{1}{d}. \tag{10}$$

However, in the case of the modified logistic map (3) a half of the preimages of $I^{(0)}$ are missing in each iteration step with respect to the case of logistic map at $r > 4$, and thus the escape rate should be by a factor of two smaller, i.e. the lifetime by a factor of two larger than in the previous case. Thus we obtain in the limit of small width d

$$\tau(d) = 2\tau_{FP}, \qquad \tau(d) = \frac{\pi\sqrt{3}}{2}\frac{1}{d}. \tag{11}$$

In Fig. 5 we present the calculated values τ in dependence on the width d (solid circles) in comparison to the prediction of Eq. (11) (solid line). As seen, for small d the theoretical prediction (11) is in excellent agreement with the calculated values of τ.

Let us now discuss the entrance of the orbits $x_n(x_0)$, $x_n(x_0 + \epsilon)$ and $x_n(x_0 - \epsilon)$, starting at x_0, $x_0 + \epsilon$ and $x_0 - \epsilon$, respectively, into the interval $I^{(0)}$.

Consider an orbit starting at $x_n(x_0)$ which enters the interval $I^{(0)}$ after exactly N_{TC} steps. In that case, there are two possibilities for the orbits $x_n(x_0+\epsilon)$ and $x_n(x_0-\epsilon)$:

(i) If the separation ϵ is sufficiently small, then both the orbits $x_n(x_0+\epsilon)$ and $x_n(x_0-\epsilon)$ would follow the orbit $x_n(x_0)$ sufficiently close, so that all three orbits enter the interval $I^{(0)}$ simultaneously, i.e. after N_{TC} steps;

(ii) With an increase of the separation ϵ between the orbits, the neighboring orbits $x_n(x_0+\epsilon)$ and $x_n(x_0-\epsilon)$ deviate more and more from the orbit $x_n(x_0)$. When the separation reaches some critical value ϵ_c, one or both of the neighboring orbits $x_n(x_0+\epsilon)$, $x_n(x_0-\epsilon)$ will not enter the interval $I^{(0)}$ simultaneously with the orbit $x_n(x_0)$. As a consequence, for $\epsilon > \epsilon_c$ the lifetime of the neighboring orbits is stochastic and $\Delta(\epsilon)$ exhibits a stochastic character.

More generally, we can discuss this problem in terms of the sensitivity of dependence of N_{TC} on the separation ϵ. In this sense we can consider a possible extension of the concept of uncertainty, which was introduced for sensitive dependence on initial conditions for fractal basin boundaries in the case of multiple attractors [26,27]. This concept was formulated for non-linear systems with multiple attractors as follows [26,27]: If the initial conditions are uncertain by an amount ϵ, for those initial conditions within ϵ of the boundary between the two attractors one could not say to which attractor the orbit eventually tends. Then the fraction $f(\epsilon)$ of initial conditions which are uncertain as to which attractor is approached when there is an initial error ϵ obeys

$$f(\epsilon) \sim \epsilon^{\alpha}, \tag{12}$$

where α is an uncertainty exponent. It has been shown that in this case the following relation holds,

$$\alpha = D - d, \tag{13}$$

where D is dimensionality of the phase space and d is the capacity dimension of the basin boundary.

Thus, in the case of multiple attractors the concept of uncertainty α is associated in predicting whether a particular orbit $x_n(x_0)$ and the neighboring orbit $x_n(x_0+\epsilon)$ will tend to the same attractor.

Let us now extend the concept of uncertainty exponent to the case of our system (3) having only one attractor. We define an uncertainty that a particular orbit $x_n(x_0)$ and a neighboring orbit $x_n(x_0+\epsilon)$ will not enter simultaneously the interval $I^{(0)}$, i.e. at the same iteration step N_{TC}. Then the fraction $f(\epsilon)$ of initial conditions which are "uncertain" as to whether the interval $I^{(0)}$ is approached simultaneously by the orbits $x_n(x_0)$ and $x_n(x_0+\epsilon)$ when there is an initial error ϵ that obeys Eq. (12).

In accordance with this new definition we have calculated the corresponding uncertainty exponent for the map (3):

$$\alpha = 0.0637 \pm 0.0005.$$

On the other hand, dimension of the asymptotic repeller of the map (3) is

$$d = 0.935 \pm 0.002.$$

As seen, these values satisfy the relation (13). This indicates that our uncertainty exponent, associated with transients in the case of a map with a single attractor, has the same property as the uncertainty exponent from Ref. [25] in the case of maps with multiple attractors.

Let us now discuss our results if we interpret ϵ as an amount by which the initial conditions are uncertain. Then it would follow that if $\epsilon < \epsilon_c$, the orbit $x_n(x_0)$ is certain with respect to the lifetime, i.e., to the iteration step N_{TC} of entering the interval $I^{(0)}$. On the other hand, if $\epsilon > \epsilon_c$ the orbit $x_n(x_0)$ is uncertain with respect to the lifetime.

It is interesting to compare computations which would employ two different computer precisions, labeled δ and δ', where δ' corresponds to the higher precision ($\delta' < \delta$). Let us first perform the computation using higher precision δ'. Suppose that we obtain a critical separation value ϵ_c which is larger than δ', but smaller than δ. In that case the result of the computation will be that an orbit $x_n(x_0)$ is certain for $\epsilon < \epsilon_c$, and uncertain for $\epsilon > \epsilon_c$. We could denote the certain orbit as the "non-chaotic" transient orbit, and the uncertain one as the "chaotic" transient orbit. Then we could say: For $\epsilon < \epsilon_c$ the transient orbit is "non-chaotic" and for $\epsilon > \epsilon_c$ it is "chaotic".

Suppose now that we perform the computation employing the lower computer precision δ. In that case

we would not have any evidence that the orbit $x_n(x_0)$ may be anything else but "chaotic".

Based on this example we can conclude that on the basis of a computer calculation, which gives always a "chaotic" transient orbit, it is not possible to decide whether the orbit is truly "chaotic" or whether there is some critical value of ϵ_c eventually lying below the level of computer precision, at which the "chaotic"-like transient turns into the "non-chaotic"-like transient.

We note that this approach could be generalized for two-dimensional maps, like, e.g. the Hénon map. In a general k-dimensional case the cumulative separation could be defined as

$$\Delta = \sum_{n=0}^{N_\infty} \tfrac{1}{2}[\,|\boldsymbol{x}_n(\boldsymbol{x}_0+\boldsymbol{\epsilon}) - \boldsymbol{x}_n(\boldsymbol{x}_0)| + |\boldsymbol{x}_n(\boldsymbol{x}_0-\boldsymbol{\epsilon}) - \boldsymbol{x}_n(\boldsymbol{x}_0)|\,]$$

with

$$\boldsymbol{x}_n = \begin{pmatrix} x_1 \\ \vdots \\ x_k \end{pmatrix}_n .$$

A generalization to dynamical systems with continuous time is possible employing

$$\Delta = \int_0^{T_\infty} \tfrac{1}{2}[\,|\boldsymbol{x}(\boldsymbol{x}_0+\boldsymbol{\epsilon}) - \boldsymbol{x}(\boldsymbol{x}_0)| + |\boldsymbol{x}(\boldsymbol{x}_0-\boldsymbol{\epsilon}) - \boldsymbol{x}(\boldsymbol{x}_0)|\,]\,\mathrm{d}t.$$

We have also extended the modified logistic map (3) to a continuous map. The results for such a more general case are similar as these presented here.

Concluding, the modification (3) of the logistic map at $r = 4$ in a narrow interval containing a low-period unstable periodic orbit leads to the stabilization of this orbit and generation of transient chaos. It is shown that this transient chaos can be well characterized by a characteristic (ϵ, Δ)-diagram: For $\epsilon < \epsilon_c$ the Δ versus ϵ dependence is given by a straight line under 45° in the log–log plot, while for $\epsilon > \epsilon_c$ a horizontal band of scattered points appears (see Fig. 3a). At the critical value of initial separation between trajectories, $\epsilon = \epsilon_c$, there is a discontinuous change of the (ϵ, Δ)-pattern.

Finally, we point out a possible extension of the concept of an uncertainty exponent to the case of transient chaos.

References

[1] T. Tel, in: Directions in Chaos, Vol. 3, ed. Hao Bai-lin (World Scientific, Singapore, 1990) p. 149.
[2] J.A. Yorke and E.D. Yorke, J. Stat. Phys. 21 (1979) 263.
[3] G. Pianigiani and J.A. Yorke, Trans. Am. Math. Soc. 252 (1979) 351.
[4] T. Shimizu and N. Morioka, Phys. Lett. A 69 (1978) 148.
[5] J. Coste, J. Stat. Phys. 23 (1980) 512.
[6] D. Ruelle, Ergod. Theor. Dyn. Syst. 2 (1982) 99.
[7] P. Manneville, Phys. Lett. A 90 (1982) 327.
[8] M. Widom, D. Bensimon, L.P. Kadanoff and S.J. Shenker, J. Stat. Phys. 32 (1983) 443.
[9] C. Grebogi, E. Ott and J.A. Yorke, Physica D 7 (1983) 181.
[10] E.N. Lorenz, Physica D 13 (1984) 90.
[11] L.P. Kadanoff and C. Tang, Proc. Natl. Acad. Sci. USA 81 (1984) 1276.
[12] S.W. McDonald, C. Grebogi, E. Ott and J.A. Yorke, Physica D 17 (1985) 125.
[13] H. Kantz and P. Grassberger, Physica D 17 (1985) 75.
[14] P. Szepfalusy and T. Tel, Phys. Rev. A 34 (1986) 2520.
[15] T. Tel, Phys. Lett. A 119 (1986) 65; Phys. Rev. A 36 (1987) 1502.
[16] T. Tel, Phys. Rev. A 36 (1987) 2507.
[17] F.M. Izrailev, B. Timmermann and W. Timmermann, Phys. Lett. A 126 (1989) 405.
[18] R. Artuso, E. Aurell and P. Cvitanović, Non-linearity 3 (1990) 325, 361.
[19] M. Franaszek, Phys. Rev. 46 (1992) 6340.
[20] A. Csordas, G. Györgyi, P. Szepfalusy and T. Tel, Chaos 3 (1993) 31.
[21] E. Ott, Chaos in dynamical systems (Cambridge University Press, Cambridge, 1993).
[22] E. Ott, C. Grebogi and A. Yorke, Phys. Rev. Lett. 54 (1990) 1196.
[23] H.G. Schuster, Deterministic Chaos (VCH, 1988).
[24] P. Cvitanović, ed., Universality in Chaos (Hilger, Bristol, 1984).
[25] H.-O. Peitgen, H. Jürgens and D. Sauppe, Chaos and Fractals (Springer, New York, 1993).
[26] C. Grebogi, S.W. McDonald, E. Ott and J.A. Yorke, Phys. Lett. A 99 (1983) 415.
[27] S.W. McDonald, C. Grebogi, E. Ott and A. Yorke, Physica D 17 (1985) 125.